

A Brief Look at *MAT_NONLOCAL: A Possible Cure for Erosion Illness?

Leonard E Schwer
Schwer Engineering & Consulting Services

Abstract

*The computational mechanics literature dealing with damage and failure is filled with work addressing what is termed mesh regularization techniques. These various techniques seek to eliminate, or minimize, the numerical artifact of strain localization. LS-DYNA[®] provides a technique for attempting to regularize meshes with damage and failure via the keyword *MAT_NONLOCAL. The non-local implementation in LS-DYNA is based on the work of Pijaudier-Cabot and Bazant (1987). The non-local treatment basically attempts to average damage/failure values of neighboring elements to minimize the mesh dependency of the results.*

The LS-DYNA non-local model uses a three-parameter weighting factor:

$$w_{ri} = w(x_r - y_i) = \left[1 + \left(\frac{\|x_r - y_i\|}{L} \right)^p \right]^{-q}$$

with two exponential parameters , and a length parameter L that determine the volume over which the average is performed. While the LS-DYNA User Manual provides 'typical' values for the exponents of $P=8$ and $Q=2$, the user needs to specify a value of the length parameter.

*In this brief look at *MAT_NONLOCAL some strategies for selecting the length parameter are investigated, and results without and with MAT_NONLOCAL are presented.*

*Those users of erosion techniques should consider adding *MAT_NONLOCAL to their simulations, as damage, and especially failure, are variants of general erosion techniques.*

Introduction

Unfortunately, the use of element erosion for penetration and perforation simulations seems to be *de rigueur* despite the existence of alternative solvers, e.g. Multi-Material ALE and SPH.

Whatever erosion criteria is selected, and however the critical value of the erosion criteria is determined, the user is responsible for demonstrating that as the mesh discretization changes, the predicted response remains the same, i.e. the result converges. When damage or failure is included in a simulation, the usual procedures for establishing mesh convergence are further complicated. The complication is the well known, see for example Belytschko 1986, that any type of strain localization phenomena, e.g. cracks, failure, strain softening (damage), will tend to localize in the smallest element in a mesh, when possible. This means for a given mesh, the smallest element in the mesh will tend to erode before the larger elements. So changing the mesh topology will lead to a different solution. i.e. non-unique solution, which is not comforting when making predictions.

The present work expands on the author's previous work (Schwer, 2009) in that the same aluminum plate perforated by an aluminum projectile is used as the illustrative example. Also, the Johnson-Cook (MAT015) constitutive model is used, with its widely expected failure criterion using the so called 'erosion strain'. The emphasis in the present work is to expand on the use of MAT_NONLOCAL to provide regularization of the Johnson-Cook constitutive model, which does not inherently consider regularization.

*MAT_NONLOCAL

The computational mechanics literature dealing with damage and failure is filled with work addressing what is termed *mesh regularization* techniques. These various techniques seek to eliminate, or minimize, the numerical artifact of strain localization. LS-DYNA provides a technique for attempting to regularize meshes with failure and damage via the keyword *MAT_NONLOCAL. The non-local implementation in LS-DYNA is based on the work of Pijaudier-Cabot and Bazant (1987). The non-local treatment basically attempts to average failure/damage values of neighboring elements to minimize the mesh dependency of the results.

The LS-DYNA non-local model uses a three-parameter weighting factor:

$$w_{ri} = w(x_r - y_i) = \left[1 + \left(\frac{\|x_r - y_i\|}{L} \right)^p \right]^{-q} \quad (1)$$

with exponential parameters p and q , and a length parameter L that determine the volume over which the average is performed. Figure 1 shows some of the weighting function variations for differing values of p and q , for a fixed length parameter $L = 2$. The LS-DYNA User Manual provides 'typical' values for the exponents of $P=8$ and $Q=2$.

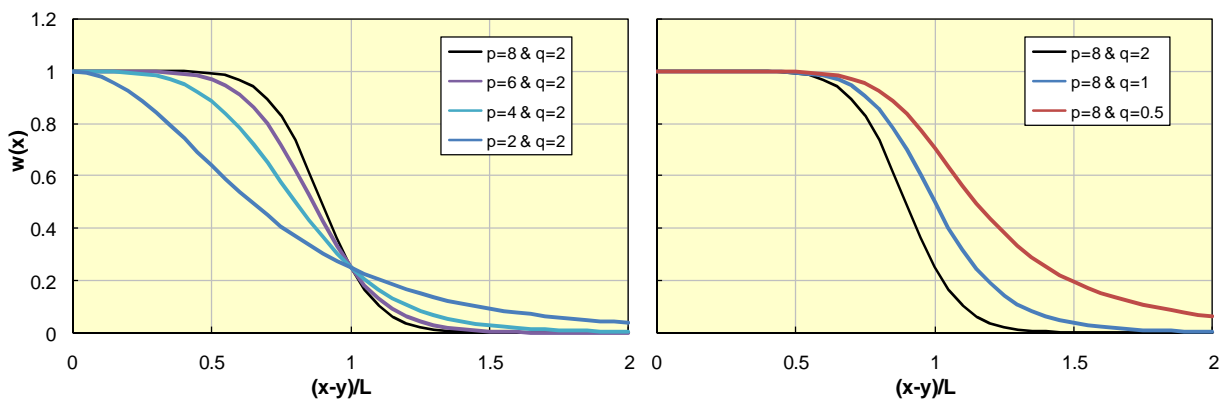


Figure 1 Illustrations of non-local weighting function variations with the parameters p and q for a fixed length parameter $L = 2$.

In addition to selecting the exponential parameters p and q , the user must select a value for the length parameter L . As shown in Figure 2, the length parameter L determines the number of

neighboring integration points to be included in forming the weighted average of the failure or damage values.

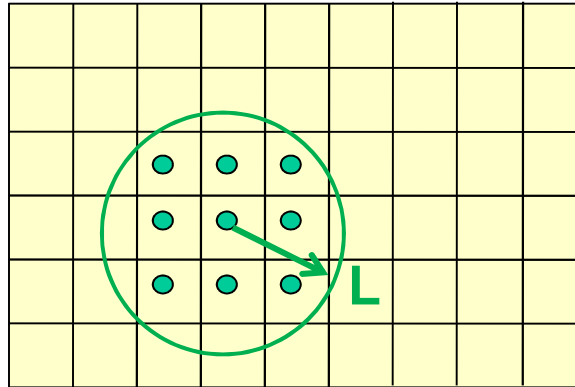


Figure 2 Schematic illustrating non-local length parameter, L , used in determining the neighboring integration points.

For a given failure or damage rate parameter \dot{d}_i , the weighted average is formed using the weighting function given by Equation (1) and the element's volume V_i , using the discrete approximation to volume integrals given by

$$\dot{d}_r \approx \frac{1}{W_r} \sum_{i=1}^{N_r} \dot{d}_i w_{ri} V_i$$

$$W_r \approx \sum_{i=1}^{N_r} w_{ri} V_i$$

The weighted average failure or damage rate parameter \dot{d}_r , is then used in the failure or damage criterion to determine the failed or damaged state of stress, to include element erosion.

Finally, since the above searching for neighboring integration points, and forming the average, is computational intensive, LS-DYNA provides a user supplied frequency parameter, NFREQ, for determining how often LS-DYNA should perform the averaging; a range of NFREQ=10 to 100 is suggested in the User Manual.

The danger of omitting regularization, when failure and damage are included in a simulation, is that the results may change with every mesh topology change, and possibly never converge under mesh refinement. Thus while regularization is highly recommended (mandatory?), the reader should recognize that the parameters p , q , L and NFREQ introduce four more *ad hoc* parameters to be joined by the typically *ad hoc* erosion criterion and its typically *ad hoc* critical value, i.e. (*ad hoc*)³ !

Illustrative Example: Aluminum Plate Perforated by an Aluminum Projectile

A series of metal plate impact experiments, using several projectile types, target materials and thicknesses, have been performed. The aluminum-on-aluminum perforation case was selected primarily because both the projectile and target were the same material, i.e. aluminum 6061-T6. Having one material simplifies the constitutive modeling, especially regarding damage and failure parameters, which is the focus of the illustrative example.

Description of the Ballistic Experiment

For the present comparative study, the only target considered is 0.5 inch (12.7 mm) thick 6061-T6 aluminum plate. The plate has a free span area of 8 by 8 inches (203 by 203 mm) and was clamped on two opposite ends.

The plate was nominally center impacted by a blunt projectile, also made from 6061-T6 aluminum, with an impact speed of 3181 feet/second (970 meters/second). The orientation of the projectile impact was intended to be normal to the target. The projectile is basically a right circular cylinder of length 0.974 inches (24.7 mm) and diameter 0.66 inch (16.7 mm), with a short length of reduced diameter (shoulder) at the rear of the projectile.

The projectile's observed exit speed was 1130 feet/second, or a 65% reduction in speed; this particular test configuration was not repeated, so an assessment of test repeatability is not available. The projectile's exit speed will serve as the primary system response quantity of interest, when comparing experimental and numerical results.

The deformed target and projectile are shown in Figure 3 and Figure 4, respectively. As can be seen the target is essentially 'drilled out' by the projectile, i.e. a clean hole remains in the target plate. Also, the minimal 'petals' on the exit surface of the target indicates the hole was formed by concentrated shear around the perimeter of the hole.



Figure 3 Side (upper image) and front (lower image) views of perforated 6061-T6 aluminum 0.5 inch thick target.



Figure 4 Deformed 6061-T6 aluminum projectiles after perforation 0.125, 0.25, and 0.5 inch thick (left-to-right) aluminum targets.

The deformed projectiles, shown in Figure 4, indicate the increasing amount of projectile deformation as it perforated increasingly thicker targets: 0.125 to 0.5 inch. The deformed projectile shown on the right is the case of present interest. The deformation of the projectile will serve as a secondary system response quantity of interest, when comparing experimental and numerical results.

Element Erosion via Johnson-Cook Failure Model

As mentioned previously, the Johnson-Cook constitutive model includes a failure criteria and a value at which the criteria erodes elements; thus two of the three aspects of using Lagrange with erosion, viz.

1. Selection of an ad hoc erosion criterion,
2. Selection of a critical value for the erosion criterion,

3. Demonstration of meshing adequacy, i.e. is the error due to discretization sufficiently small.

are addressed automatically when the Johnson-Cook failure model is used. The third aspect applies to all forms of numerical simulations that involve space and/or time discretization.

Mesh Refinements

Five mesh refinement models were constructed for use with the two-dimension axisymmetric solver in LS-DYNA. While the three-dimensional solver could also be used, use of the two-dimension axisymmetric solver allows for more efficient solutions, especially with a large number of elements. Figure 5 shows the coarsest of the five axisymmetric mesh configurations. The mesh discretizations are similar in that each mesh uses one number as the basis for determining the number and size of all the elements in the mesh. The base number is the number of elements through the radial thickness of the shoulder region at the aft end of the projectile. This thickness is 1.778 mm and the coarsest mesh, shown at the top of Figure 5, uses two elements across this shoulder dimension, and is designated as “Mesh 2S,” just to assign a name. The particulars of the five meshes are summarized in Table 1. The mesh refinement level doubles in the first two cases, i.e. 4S and 8S, then increase by a factor of 1.5 for the 12S mesh, and finally the 16S mesh is a factor of 1.33 more refined then the 12S mesh. Note: The mesh sequence 2-4-8-16S are all mesh doublings.

Table 1 Summary of mesh configurations for erosion simulations.

Mesh	Smallest Element (mm)	Number of Elements
2S	0.889	811
4S	0.4445	3,174
8S	0.22225	12,913
12S	0.14816	28,922
16S	0.111125	51,691

The overall projectile and target plate dimensions were given above in the description of the ballistic experiment. The target plate elements immediately below the projectile have the same mesh refinement as the projectile. From the projectile diameter to mid-radius of the target plate There is a coarsening of the mesh via a geometric ratio of the element sizes. The outer most portion of the plate uses a constant element size equal to the last geometric ratio element size.



Figure 5 Coarsest of the five axisymmetric mesh discretization considered for the Lagrange with erosion simulations designated 2S.

Results – Projectile Residual Speeds and Eroded Elements

Table 2 provides a summary of the projectile residual speeds for the five mesh refinements considered, when element erosion, via the Johnson-Cook failure criterion, is included. The projectile speeds are decreasing with increasing mesh refinement, however not monotonically, i.e. for the two finest meshes (12S & 16S) the speed is increasing and greater than the speed for the 8S mesh.

Figure 6 shows a plot of the residual speed versus the mesh refinement size parameter. This plot makes it clear that the results appear (visual convergence criteria?) to be in the asymptotic regime. However the apparent value to which the results are converging, i.e. about 1500 fps, is about 35% greater than the experimental residual speed of 1103 fps.

Table 2 Summary of projectile residual speeds for Lagrange with erosion.

Mesh	Smallest Element (mm)	Residual Speed (fps)
2S	0.889	1874
4S	0.4445	1743
8S	0.22225	1659
12S	0.14816	1718
16S	0.111125	1742
Experiment		1103

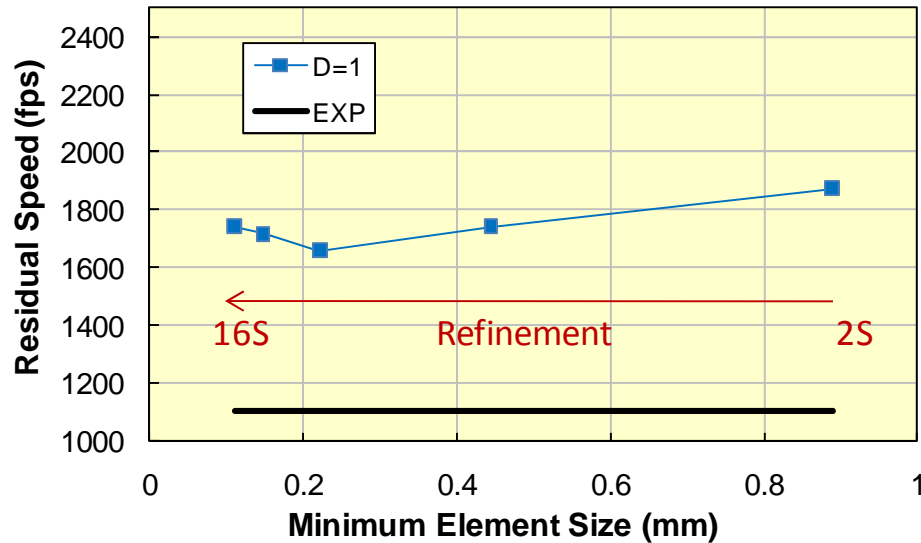


Figure 6 Residual projectile speed versus mesh refinement parameter.

Figure 7 provides a graphic indication of the elements which are eroded during the simulation; the eroded elements are shown relative to their initial configuration and indicated by a different color to differentiate them from the non-erode elements of the same part. A visual inspection of these images indicates that a decreasing volume of material is eroded with decreasing mesh size (increasing in mesh refinement). This visual assessment is quantified in Figure 8 which plots the ratio of the total energies without and with the eroded elements, e.g. $(\text{Total Energy} - \text{Total Energy of Eroded Elements}) / \text{Total Energy}$. This ratio transitions from a minimum of 47% for the 2S mesh to 69% for the 12S mesh, i.e. the total energy of the eroded elements is decreasing with increasing mesh refinement, except the finest mesh (16S) has the same erode energy ratio as the 8S mesh, but a somewhat different pattern of eroded elements.

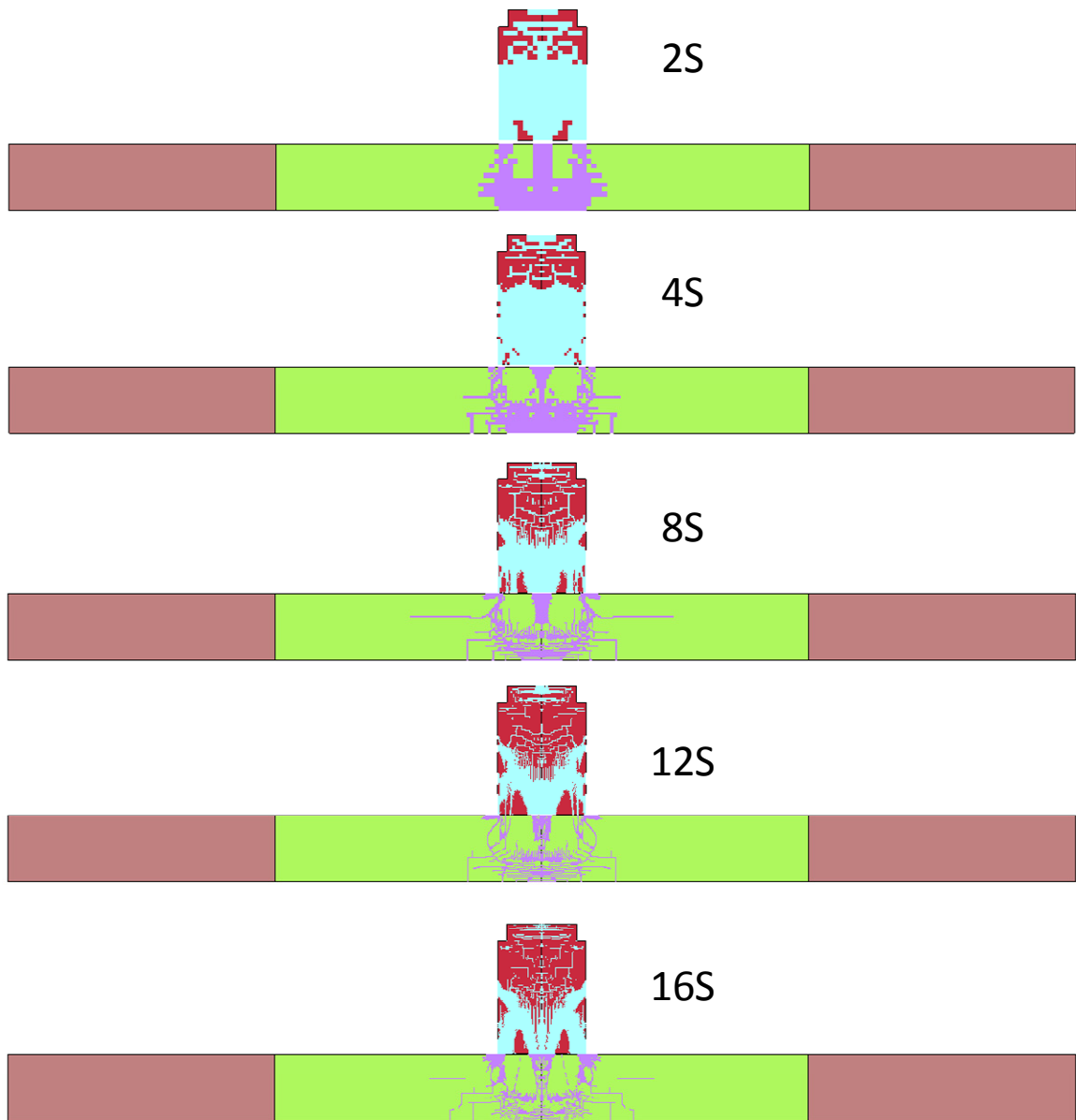


Figure 7 Graphic indication of the elements that are eroded in the projectile and plate.

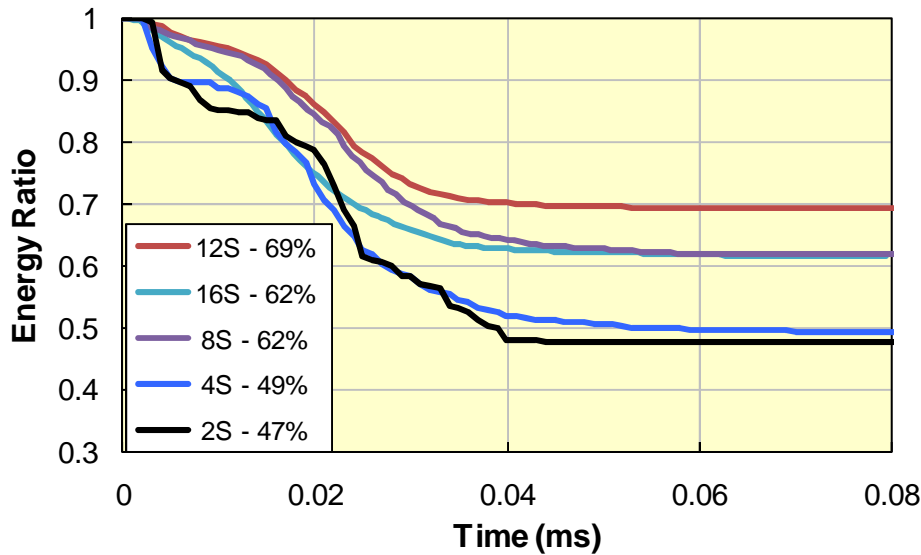


Figure 8 Ratio of total energies without and with eroded elements.

Results with Regularization

The above results for Lagrange with erosion did not include mesh regularization, and obviously showed a mesh size dependency, in terms of the projectile residual speed and especially in the amount of material eroded from both the projectile and target. In this section, mesh regularization is included in the simulations using the LS-DYNA keyword *MAT_NONLOCAL. The parameters required for the *MAT_NONLOCAL averaging, recall Equation (1), were taken from the LS-DYNA User Manual provided ‘typical’ values for the exponents, $P=8$ and $Q=2$, with two fixed values of the length parameter, i.e. $L = 2$ and 4 , and a variable length explained below.

These two fixed values of the *MAT_NONLOCAL length parameter will include an increasing number of adjacent integration points as the mesh is refined. If we define a nondimensionalized length parameter: $\bar{L} = L / L_{ele}$ where L_{ele} is the nominal element dimension, then we can estimate the number of integration points for each mesh refinement as $Int(\bar{L})^2$, i.e. the integer value of \bar{L} squared, for the present two dimensional simulations. Table 3 provides this estimate of the number of integration points for the two selected fixed length parameters for the four¹ mesh refinements. Obviously, the number of integration points rapidly becomes large using this approach; also the corresponding CPU time and memory requirements increase rapidly. Further, in three dimensions, where the *cube* of the normalized length parameter would be used to estimate the number of integration points, the computer resources required rapidly exceed practical limits.

However, this fixed length parameter approach is the one often recommend in the literature, see for example Pijaudier-Cabot & Z.P. Bazant (1987), as the length is thought of as representing some physical characteristic of the material that is failing. As an example, in concrete model

¹ The 16S mesh is no longer considered in the remainder of the document.

simulations, a multiple of the average aggregate size, e.g. three times the aggregate diameter, is typically recommended. For metals, no such convenient physical dimensional parameter exists.

Table 3 Estimated number of integration points for each mesh with a fixed averaging length.

MESH	L_{ele}	$Int(\bar{L})^2$	
		$L = 2$	$L = 4$
2S	0.889	4	16
4S	0.4445	16	64
8S	0.22225	64	289
12S	0.148167	169	676

The other possible approach to selecting the length parameter during mesh refinement, is to keep the number of surrounding integration points approximately constant as the mesh is refined, i.e. a variable length parameter. In a 2D regular rectangular mesh, the eight neighboring integration points will lie inside a circle of radius $\sqrt{2}L_{ele}$, where L_{ele} is the element characteristic length. For a 3D regular mesh the 26 nearest integration points will be inside a sphere of radius $\sqrt{3}L_{ele}$. Thus for the 2S mesh

$$L = \sqrt{2}L_{ele} = \sqrt{2}(0.889) = 1.257 \sim 2.0$$

Here the approximate value 2.0 is used for convenience, as this value was also used as a fixed length parameter. For the 4S, 8S, and 12S mesh, the variable length parameters are 1.0, 0.5, and 0.333 respectively.

To activate *MAT_NONLOCAL in LS_DYNA requires two additional keywords: *CONTROL_NONLOCAL and *MAT_NONLOCAL. The former keyword provides for some additional internal storage (memory) and its only parameter is the recommended value of MEM=10 as per the LS-DYNA User Manual.

```
*CONTROL_NONLOCAL
$ MEM
  10
$
*MAT_NONLOCAL
$ IDNL  PID  P  Q  L  NFREQ
   1,  40,  8,  2,  2.0,  10
$ NL1  NL2  NL3  NL4  NL5  NL6  NL7  NL8
   6,   0,   0,   0,   0,   0,   0,   0
$ XC1  YC1  ZC1  XC2  YC2  ZC2
   0.0,  0.0,  0.0,  1.0,  0.0,  0.0
$
```

The main input parameters for the *MAT_NONLOCAL keyword are:

- PID – LS-DYNA part number to which *MAT_NONLOCAL is to be applied,
- P, Q, L – parameters used in weighted average, refer back to Equation (1).
- NFREQ – number of time steps between application of *MAT_NONLOCAL average,

- NL – memory location of history variables to be averaged, refer to the table in the LS-DYNA User Manual under the keyword *MAT_NONLOCAL,
- XC, YC, ZC – vectors defining any symmetry planes associated with the PID.

Results with Regularization – Initial Results

Initial projectile perforation simulations with MAT_NONLOCAL produced unexpected results. As shown in Figure 9 for the 2S mesh with L=2, highly elongated elements of the target plate were not failed by the regularized Johnson-Cook criterion. These ‘tendrils’ from the target plate acted as a drag on projectile, greatly reducing the residual speed; see Figure 10. Worse, these high aspect ratio elements caused the minimum time step to decrease by about an order of magnitude. Eventually, for the 8S and L=4 case, the simulation aborted due to a negative time step calculation for one of the highly distorted elements.

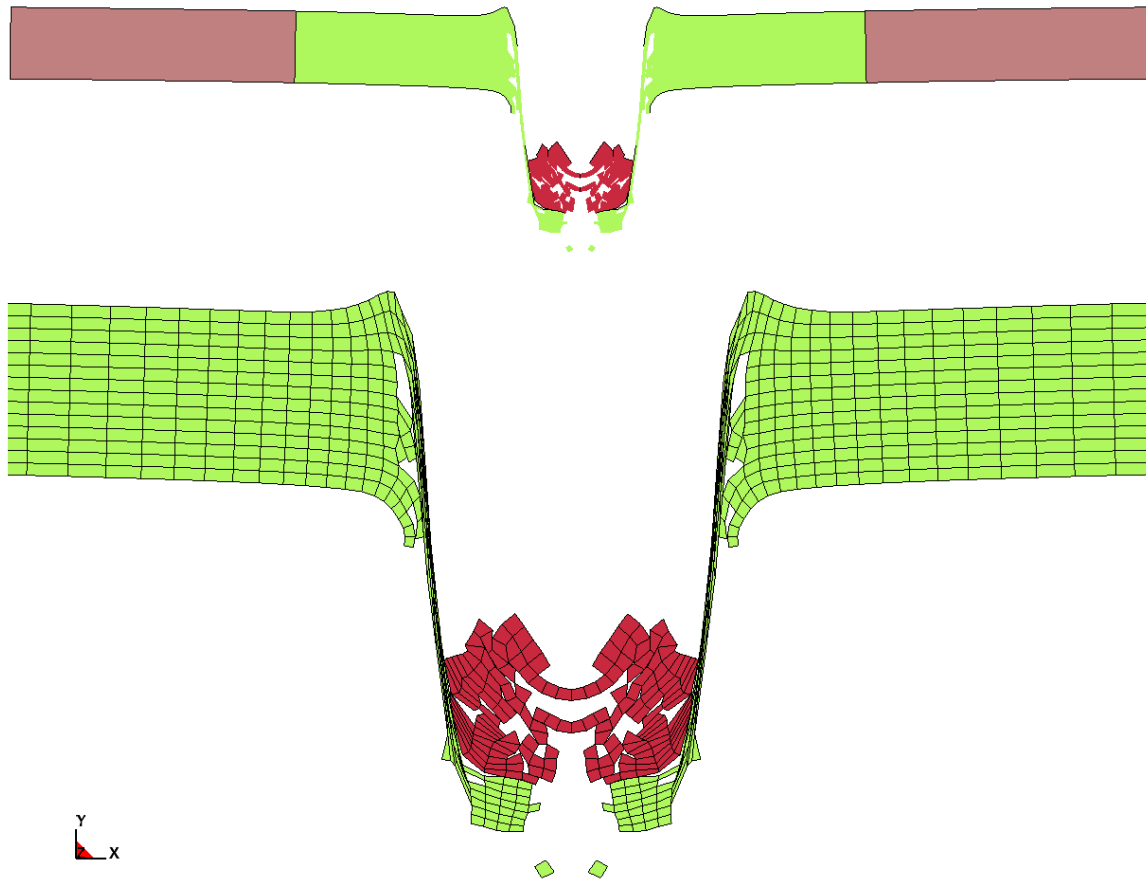


Figure 9 Initial application of MAT_NONLOCAL for the 2S mesh with L=2.

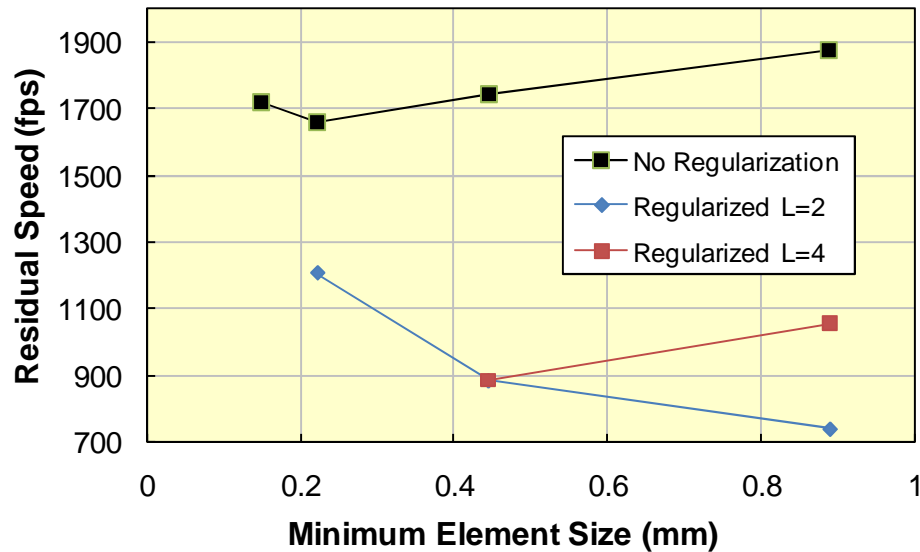


Figure 10 Projectile residual speed for initial application of MAT_NONLOCAL.

Results with *MAT_ADD_EROSION and EPSSH

Obviously these highly deformed target elements also needed to be eroded from the simulations, to continue with the comparisons. Since there is no general method for eliminating shell elements, this includes 2D plane stress/strain and axisymmetric solids (present case), based on a minimum time step in LS-DYNA, it was decided to use the *MAT_ADD_EROSION keyword with a maximum shear strain criterion (EPSSH) for erosion of the troublesome target plate shell elements.

The *MAT_EROSION keyword requires an associated material ID (MID) for application of the erosion criteria, and a value for one or more of its predefined defined erosion criteria; in the present case EPSSH=1.0 or a shear strain of 100%. Again, the reader is reminded this criterion, and its value, are *ad hoc*.

```

$
*MAT_ADD_EROSION
$ MID EXCL MXPRESS MNEPS EFFEPS VOLEPS NUMFIP NCS
  6061, 666
$ MNPRES SIGP1 SIGVM MXEPS EPSSH SIGTH IMPULSE FAILTM
  666, 666, 666, 666, &EPSSH, 666, 666, 666
$

```

The exclusion parameter, EXCL=666, in the *MAT_ADD_EROSION keyword allows the user to specify criteria to be ignored, that have no default value, without ambiguity.

The inclusion of the *MAT_ADD_EROSION maximum shear strain in the perforation simulations requires repeating the previous simulations without regularization, to establish new baseline values for comparison with the regularized results. Table 4 provides a comparison of the projectile residual speeds for the four mesh refinements using the Johnson-Cook (D=1) failure criterion, as provided previously in Table 2, and the corresponding results when the maximum

shear strain criterion (EPSSH=1) is included. The projectile speeds with EPSSH=1 are decreasing monotonically with increasing mesh refinement.

Table 4 Summary of projectile residual speeds for Lagrange with erosion.

Mesh	Residual Speed (fps)	
	D=1	D=1 & EPSSH=1
2S	1874	2385
4S	1743	1792
8S	1659	1681
12S	1718	1621
Experiment	1103	

Figure 11 compares the projectile residual speeds for the four mesh refinements using the Johnson-Cook D=1 erosion criterion with and without the addition of the maximum shear strain (EPSSH=1) criterion. This plot makes it clear that the D=1 and EPSSH=1 results are not in the asymptotic regime, and that further mesh refinement is suggested. However, further mesh refinement may not produce results in an asymptotic regime. In part, the results may not be converging with mesh refinement because the erosion of elements causes ‘jumps’ in the mesh and thus discontinuities. In the next section, an attempt to make the results more continuous, via *MAT_NOLOCAL, is demonstrated.

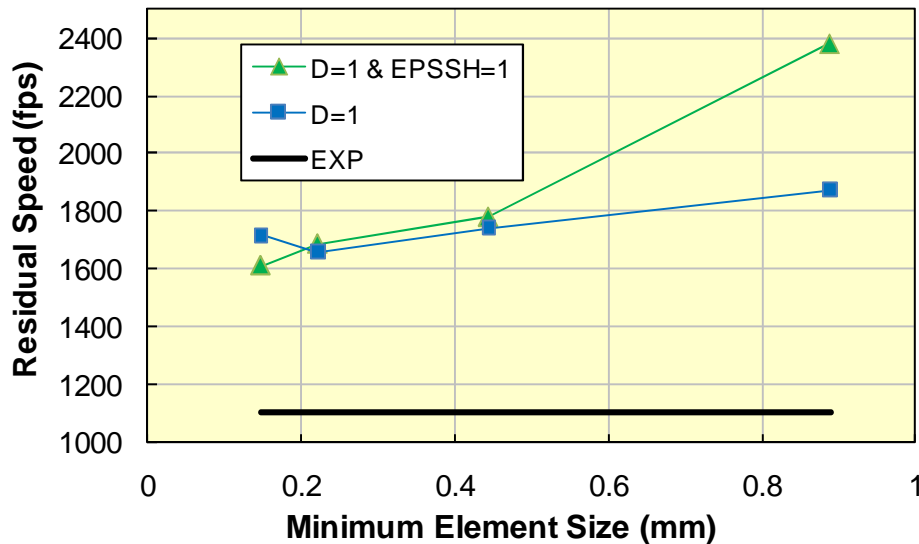


Figure 11 Comparison of projectile residual speeds for the Johnson-Cook erosion (D=1) with and without the addition of the maximum shear strain (EPSSH=1) criterion.

Results with Regularization and *MAT_ADD_EROSION

Table 5 presents a comparison of the projectile residual speeds for four mesh refinements without and with mesh regularization via *MAT_NONLOCAL, all results include MAT_ADD_EROSION using EPSSH=1. The results listed under the heading “No Regularization” where previously presented in Table 4 and Figure 11. The same comparison of without and with

regularization results is shown in graphical form in Figure 12. In this figure it is easy to see that the addition of *MAT_NONLOCAL does not influence the projectile residual speed significantly. However, unlike the no regularization case, projectile residual speeds with regularization appear to be in the asymptotic regime, as the two finest mesh results, i.e. 8S and 12S, have nearly identical residual speeds.

Table 5 Summary of projectile residual speeds for Lagrange with erosion without/with regularization.

Mesh	Smallest Element (mm)	Residual Speed (fps)		
		No Regularization	$L = 2$	$L = 4$
2S	0.889	2385	2469	2396
4S	0.4445	1792	1699	1685
8S	0.22225	1681	1672	1610
12S	0.14816	1621	1659	1630
Experiment		1103		

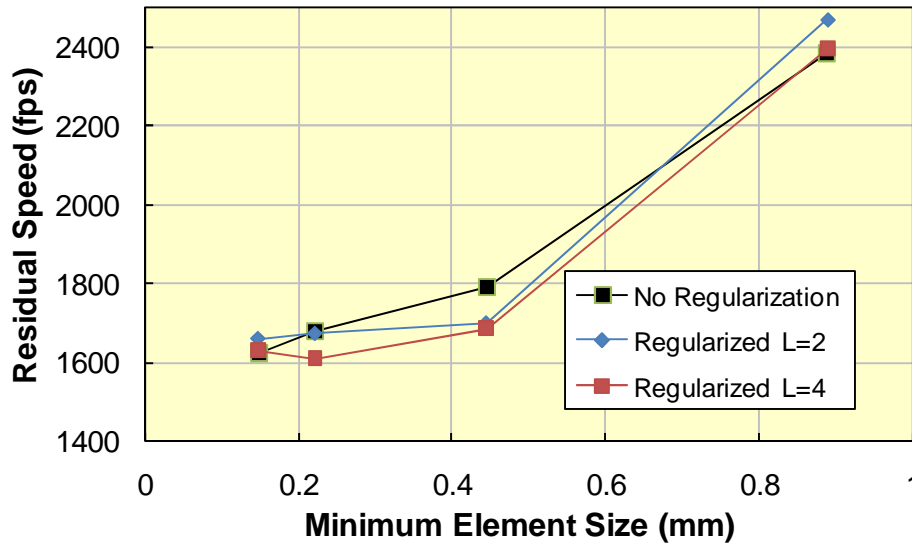


Figure 12 Comparison of projectile residual speed versus mesh refinement without/with regularization via *MAT_NONLOCAL.

These regularized results indicate the mesh refinement results are converging, but converging to a speed that is not the same as was observed in the experiment. Convergence of results is a desirable trait in any simulation, but it is no guarantee the converged answer is the ‘correct’ answer. Some additional confirmation that the simulation produces results different from the experiment is shown in Figure 13 where the final shape of the projectile from the 8S simulation is compared with the projectile recovered from the experiment. While the shapes are similar, there is obviously material missing from the simulated projectile that is present in the projectile from the experiment. In particular, the recovered projectile’s aft region, including the shoulder is intact, while that portion of the simulated projectile is distorted due to the erosion of material in the center rear of the simulated projectile.

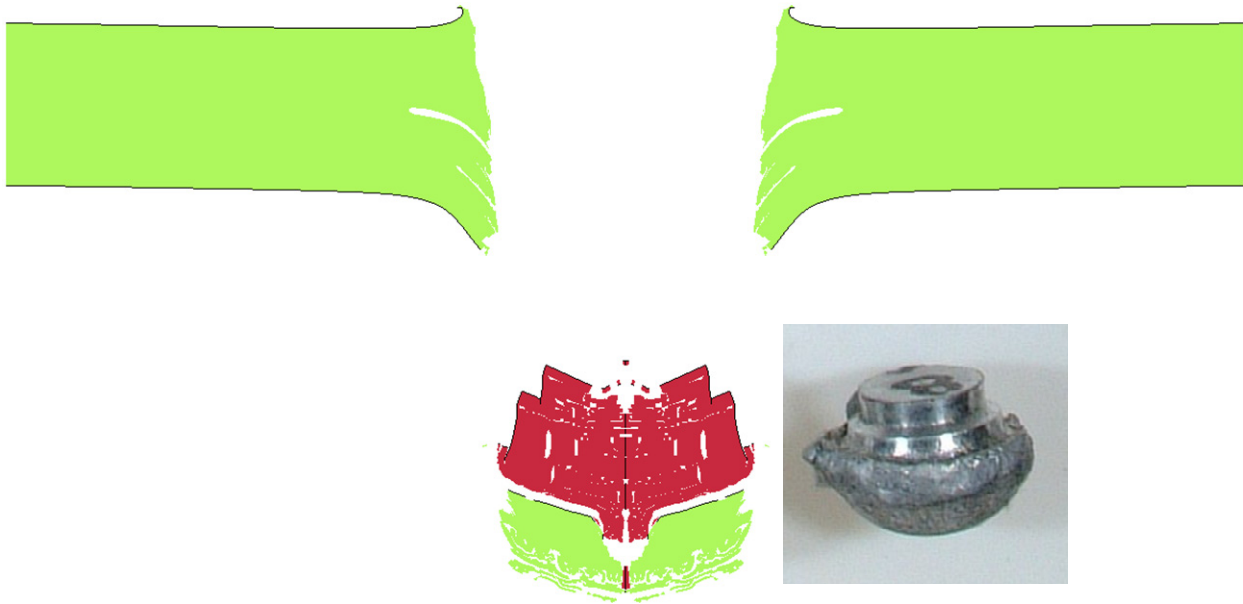


Figure 13 Comparison of deformed projectiles from 8S (L=2) simulation and experiment.

As discussed above, the choice of the length parameter when using MAT_NONLOCAL is for the most part *ad hoc*, unless the material possesses some inherent length scale, e.g. aggregate size in concrete. In the previous MAT_NONLOCAL results two length parameters were selected for comparison, i.e. $L=2$ and $L=4$, and the decision was made to hold these length parameters constant during the mesh refinement studies. The results, shown previously in Table 5 and Figure 12, indicate only small changes in the predicted projectile residual speed for these two choices of the length parameter. An additional length parameter study was conducted using a variable length parameter that maintained approximately the same number of neighboring integration points as the mesh was refined. Table 6 and Figure 14 include the projectile residual speed results when the variable length parameter is included. Again, the results with the variable length parameter are similar to those with the two fixed length parameters. However, the CPU time for the more refined meshes, i.e. 8S and 12S, was only 20% and 9%, respectively, the CPU required for the $L=2$ constant mesh refinements study. The conclusion in this part of the study is that the variable length parameter is a more efficient choice than a fixed length parameter.

Table 6 Summary of projectile residual speeds for Lagrange with erosion without/with regularization.

Mesh	Smallest Element (mm)	Residual Speed (fps)			
		No Regularization	$L = 2$	$L = 4$	Variable
2S	0.889	2385	2469	2396	2469 (L=2)
4S	0.4445	1792	1699	1685	1803 (L=1)
8S	0.22225	1681	1672	1610	1624 (L=0.5)
12S	0.14816	1621	1659	1630	1671 (L=0.33)
Experiment		1103			

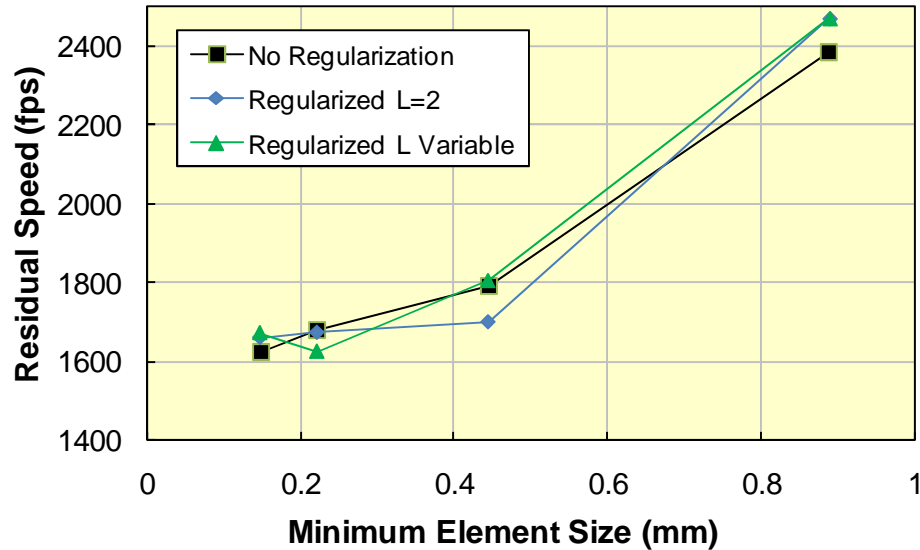


Figure 14 Comparison of projectile residual speed without regularization, constant L=2 and variable regularization.

Finally, the choice of $EPSSH=1.0$ is also recognized to be *ad hoc*. Two additional `MAT_NONLOCAL` parameter studies were performed using values of $EPSSH=0.5$ and 1.5 with the 8S mesh. The residual speed results for this parameter study are shown in Table 7. This limited parameter study indicates a dependence of the residual projectile speed on the value of $EPSSH$, but again the results do not indicate a converging pattern.

Table 7 Residual projectile speeds for $EPSSH$ parameter study.

$EPSSH$	Residual Speed (fps)
0.5	1889
1.0	1624
1.5	1663

Summary

This work demonstrates performing simulations of metal plate perforation via Lagrange with erosion, and has focused on using mesh refinement studies to examine the behavior of various forms of Lagrange with erosion. The forms examined include:

- Erosion using Johnson-Cook failure criterion and failure strain parameter,
- Augmentation of the Johnson-Cook failure with `*MAT_ADD_EROSION`,
- Regularization of the failure parameter using `*MAT_NONLOCAL`.

The main points discussed and illustrated in this study are:

- Erosion requires the selection of several *ad hoc* parameters. Chief among these are the erosion criterion and its value. By using the Johnson-Cook failure criterion and failure strain parameter, these two critical choices were avoided, but for most other constitutive models this will not be the case. Because the Johnson-Cook constitutive model is both appropriate for the problem at hand, i.e. metal plate perforation, and provides a

predefined failure criterion and value at failure, this paper was able to focus on the other factors affecting solutions using Lagrange with erosion; these factors are listed next.

- Mesh refinement is mandatory in all computational mechanics simulations. Without at least one, or preferably two alternative meshes, no estimate of the discretization error can be obtained.
- Mesh refinement in the presence of damage or failure can be problematic, as the damage or failure tends to localize in the smallest elements in a mesh. To minimize this localization affect, regularization techniques, such as *MAT_NONLOCAL are used in an effort to reduce mesh size sensitivity. The use of *MAT_NONLOCAL adds three more *ad hoc* parameters to the simulation. For the present example, it was illustrated that for the length parameter in *MAT_NONLOCAL, there was not much sensitivity to the choice of this parameter. Undemonstrated are the sensitivity of the weighting functions parameters p and q.
- The introduction of *MAT_NONLOCAL caused an unanticipated problem of allowing elements with high aspect ratios to remain in the calculation beyond where the Johnson-Cook failure model would have removed them. To eliminate these troublesome high aspect ratio elements, another erosion criterion was added, i.e. the maximum shear strain via *MAT_ADD_EROSION. The choice of the maximum shear strain and its value for erosion, EPSSH=1.0, are also *ad hoc*. The value of this erosion criteria also affects the solution, and as illustrated for the present example, does not produce results, i.e. projectile residual speeds, that change monotonically with the value of the maximum shear strain.

References

Belytschko, T., Z.P. Bazant, Y-W. Hyun and T.-P. Chang, "Strain Softening Materials and Finite Element Solutions," Computers and Structures, Volume 23, Number 2, pages 163-180, 1986.

Pijaudier-Cabot, G and Z.P. Bazant, "Nonlocal Damage Theory," Journal of Engineering Mechanics, ASCE, Volume 113, Number 10, pp. 1512-1533, 1987.

Schwer, L.E., "Aluminum Plate Perforation: A Comparative Case Study Using Lagrange With Erosion, Multi-Material ALE, and Smooth Particle Hydrodynamics," 7th European LS-DYNA Conference, Salzburg, Austria, 2009.
http://www.dynalook.com/european-conf-2009/J-I-01.pdf/at_download/file